ARTICLE

OPEN

Check for updates

Dissipation-driven strange metal behavior

Sergio Caprara [1,2,4✉], Carlo Di Castro[1], Giovanni Mirarchi[1], Götz Seibold [3] & Marco Grilli [1,2,4✉]

Anomalous metallic properties are often observed in the proximity of quantum critical points, with violation of the Fermi Liquid paradigm. We propose a scenario where, near the quantum critical point, dynamical fluctuations of the order parameter with *finite correlation length* mediate a nearly isotropic scattering among the quasiparticles over the entire Fermi surface. This scattering produces a strange metallic behavior, which is extended to the lowest temperatures by an increase of the damping of the fluctuations. We phenomenologically identify one single parameter ruling this increasing damping when the temperature decreases, accounting for both the linear-in-temperature resistivity and the seemingly divergent specific heat observed, e.g., in high-temperature superconducting cuprates and some heavy-fermion metals.

[1] Dipartimento di Fisica, Sapienza Università di Roma, P. le Aldo Moro 5, 00185 Roma, Italy. [2] ISC-CNR, Unità di Roma Sapienza, P. le Aldo Moro 5, 00185 Roma, Italy. [3] Institut für Physik, BTU Cottbus-Senftenberg - PBox 101344, D-03013 Cottbus, Germany. [4] These authors jointly supervised: Sergio Caprara, Marco Grilli. ✉email: sergio.caprara@roma1.infn.it; marco.grilli@roma1.infn.it

Landau's Fermi liquid (FL) theory is one of the most successful paradigms in condensed matter physics and usually describes very well the prominent properties of metals even when the interaction is strong, like, e.g., in heavy-fermion metals or in the normal (non-superfluid) phase of ^{3}He. However, in the last decades, a wealth of systems violating the paradigmatic behavior has been discovered. In particular, it has been noticed that in several different materials, like heavy fermions metals[1], iron-based superconductors[2], organic metals like $(TMTSF)_2PF_6$, high-temperature superconducting cuprates (for an extended analysis of several materials see refs. [3,4]), a non-FL behavior can occur in the proximity of quantum critical points (QCPs), i.e., near zero-temperature second-order phase transitions, where the uniform metallic state is unstable towards some ordered state. It is worth mentioning that, apart from the paradigmatic case of the one-dimensional Luttinger liquid, there are also theories for the violation of the FL behavior that do not rely on an underlying criticality[5,6]. In some cases, like in high-temperature superconducting cuprates (henceforth, cuprates), the ordered state may be unaccomplished due to disorder, low dimensionality, and/or competition with other phases, like superconductivity. Nevertheless, the non-FL behavior is observed also in these cases of missed quantum criticality, showing that a mere tendency to order and the presence of abundant order parameter fluctuations (henceforth, fluctuations) may be sufficient to create a non-FL state. The general underlying idea is that the fluctuations are intrinsically dynamical, with a characteristic energy m becoming smaller and smaller as the correlation length ξ grows larger and larger, when the QCP is approached. In the paradigmatic case of a Gaussian QCP in a metal, with a dynamical critical index $z = 2$, the retarded propagator of the fluctuations with wavevector $\mathbf{q}$ and frequency ω is[7–10]

$$D(\mathbf{q}, \omega) = \left(m + \bar{\nu}|\mathbf{q} - \mathbf{q}_c|^2 - \omega^2/\overline{\Omega} - i\gamma\omega \right)^{-1}, \qquad (1)$$

where $m = \bar{\nu}\xi^{-2}$ is the mass of the fluctuations, $\bar{\nu}$ is typically an electron energy scale [we work with dimensionless momenta, measured in reciprocal lattice units (r.l.u.) $2\pi/a$], $\mathbf{q}_c$ is the critical wavevector, and $\overline{\Omega}$ is a frequency cutoff. A crucial role in the following will be played by the imaginary term in the denominator, which describes the Landau damping of the fluctuations, as they decay in particle-hole pairs. The dimensionless parameter γ is usually proportional to the electron density of states, which sets a measure of the phase space available for the decay of the fluctuations. It is worthwhile mentioning that the strong correlations of the metal are customarily encoded in a renormalization of the quasiparticle mass and of the effective residual interaction, e.g., within a slave-boson approach[10–12]. Once these effects are taken into account, a random-phase approximation within the renormalized FL works well to describe the instabilities of the FL, e.g., towards a charge-ordered state, which is a well-established tendency of cuprates, where a wealth of nearly critical and less critical fluctuations have been experimentally detected[13]. Of course, other modes like plasmons and paramagnons mark the spectra of these systems at high energies (some hundreds of meV), where correlation effects surely play a substantial role[14,15], but here we are mostly interested in the low-energy physics of transport phenomena. In this regime the fermionic quasiparticles mostly interact with low-energy collective excitations with a slow overdamped dynamics mostly determined by the proximity to (more or less hidden) instabilities. In two dimensions and for a dynamical critical index $z = 2$ (as appropriate to Landau-damped collective modes) these low-energy modes are well described by the Gaussian form of the fluctuation propagator reported in Eq. (1). Clearly, in the Gaussian case, for $\omega = 0$ and $\mathbf{q} \approx \mathbf{q}_c$ one obtains the standard Ornstein–Zernike form of the static

susceptibility. The same behavior of the fluctuations can be obtained within a time-dependent Landau–Ginzburg approach, where γ is the coefficient of the time derivative and the decay rate of the fluctuations is given by $\tau_{\mathbf{q}}^{-1} = (m + \bar{\nu}|\mathbf{q} - \mathbf{q}_c|^2)/\gamma$.

Approaching the QCP, ξ grows, m decreases and the fluctuations become softer and softer, thereby mediating a stronger and stronger interaction between the fermion quasiparticles (henceforth, simply quasiparticles). In two and three dimensions the interaction could be strong enough to destroy the FL state[16]. For ordering at finite wavevectors, though, there is a pitfall in this scheme[17]: due to momentum conservation, this singular low-energy scattering only occurs between quasiparticles near points of the Fermi surface that are connected by $\mathbf{q} \sim \mathbf{q}_c$ (hot spots). All other regions are essentially unaffected by this singular scattering and most of the quasiparticles keep their standard FL properties. As a result, for instance, in transport, a standard FL behavior would occur, with a T^2 FL-like resistivity[17]. Disorder may help to blur and enlarge the hot regions[18], but it does not completely solve the above difficulty. Of course, this limitation does not occur in cases where $\mathbf{q}_c = \mathbf{0}$ (like, e.g, near a ferromagnetic[19], or a circulating-current[20], or a nematic[21] QCP), or near a local QCP (i.e., when the singular behavior persists locally for all $\mathbf{q}$)[22–25]. However, the very fact that similar non-FL behavior also occurs near QCPs with finite $\mathbf{q}_c$ calls for a revision of the above scheme searching for a general and robust way to account for non-FL phases irrespective of the ordering wavevector.

The main goal of the present work is to describe an alternative scenario for the non-FL behavior, based on the idea that the decay rate of the fluctuations $\tau_{\mathbf{q}}^{-1}$ becomes very small not only at $\mathbf{q} \approx \mathbf{q}_c$, because of a diverging ξ, but rather at all $\mathbf{q}$'s, because of a (nearly) diverging γ, as T goes to zero at special values of the control parameter as, e.g., doping in cuprates. We will adopt a phenomenological approach and we will explicitly show that a finite ξ and a large γ are generic sufficient conditions to obtain the most prominent signatures of non-FL strange-metal behavior: a linear-in-temperature (T) resistivity (even down to very low temperature) and a (seemingly) diverging specific heat. For the sake of concreteness, we will consider the paradigmatic case of cuprates, where at some specific doping both features are observed[3,26], having in mind that they also commonly occur in many other systems like, e.g. heavy fermions[1]. This suggests that our proposal might have a broad applicability.

Results and discussion

Dissipation-driven strange metal behavior. The above scenario can be achieved on the basis of three simple and related ingredients: (a) The proximity to a QCP, bringing the fluctuations to sufficiently low energy; (b) Some quenching mechanism preventing the full development of criticality so that the mass m and the other parameters of the dynamical fluctuations do not vary in a significant way with temperature; (c) Some mechanism driving an increase of the Landau damping parameter γ. Indeed the non-FL behavior persists down to a temperature scale $T_{FL} \sim \omega_0 \equiv m/\gamma = \bar{\nu}/(\xi^2\gamma) = \tau_{\mathbf{q}_c}^{-1}$ when ξ is finite and not particularly large. In cuprates, recent resonant X-ray scattering (RXS) experiments[13] show that conditions (a) and (b) hold: the occurrence of a temperature dependent narrow peak due to charge density waves testifies the proximity to a QCP (although hidden and not fully attained due to the competition with the superconducting phase). The concomitant occurrence of broad peak witnesses for the presence of dynamical charge density fluctuations (CDFs) with rather short correlation length and broad momentum distribution. These abundant CDFs are available to isotropically scatter the quasiparticles over a broad range of momenta and no clear distinction can be done between hot and cold Fermi surface

regions[27]. This was the first explicit example that a quenched criticality with a finite ordering wavevector $\mathbf{q}_c$ can still give rise to strong but isotropic scattering, thereby bypassing the problem that in standard hot spot models most electrons contribute with a $\sim T^2$ scattering rate to transport[17]. This shows that conditions (a) and (b) are enough to account for a linear-in-T resistivity above T_{FL}. Condition (c) becomes instead mandatory because an increasing γ is needed to extend to lower temperatures the non-FL behavior, accounting for the persistence of the linear resistivity observed down to a few Kelvins, which is the so-called strange-metal behavior, sometimes also referred to as the Planckian behavior[3,28] (for a distinction between the strange-metal and the Planckian behavior, see below), as well as a seemingly diverging specific heat[26,29] (see below).

To address this issue, we investigate the effects of an increasing γ on the fluctuations, which provide both a broad scattering mechanism for resistivity and low-energy excitations for the specific heat. From the retarded propagator we obtain the spectral density of the fluctuations[11,30–32]

$$\text{Im } D(\mathbf{q}, \omega) = \frac{\gamma\omega}{\left(m + \bar{\nu}|\mathbf{q} - \mathbf{q}_c|^2 - \omega^2/\overline{\Omega}\right)^2 + \gamma^2\omega^2},$$

which, for $\mathbf{q} = \mathbf{q}_c$, is maximum at $\omega \approx \omega_0 \equiv m/\gamma$. For large γ (whatever the reason), ω_0 is much smaller than m and sets the characteristic energy scale of the dynamical fluctuations. As mentioned above, a large γ suppresses the energy scales associated with $\tau_{\mathbf{q}}^{-1}$ at all $\mathbf{q}$'s [One could even argue that when this slow dynamics of the small droplets of the fluctuations (of order ξ) is reached, a kind of almost persistent glassy state is likely formed].

Figure 1 (a) and (b) display this shift to lower frequencies of $b(\omega) \text{ Im } D(\omega)$ and $\text{Im } D(\omega)$ when γ increases [$b(\omega) = (e^{\omega/T} - 1)^{-1}$ being the Bose function]. Panel (c) schematically shows the corresponding extension of the linear resistivity down to lower and lower temperatures. Indeed, although the collective fluctuations obey the Bose statistics, at any temperature $T > \omega_0$ they acquire a semiclassical character and their thermal Bose distribution becomes linear in T, $b(\omega) \approx T/\omega$. Notice that this is the usual situation for phonons when T is above their Debye temperature. The only difference here is that a small/moderate m (due to the proximity to a QCP) and the large γ conspire to render the Debye scale of the fluctuations particularly small or even vanishing if γ may diverge, while m stays finite. Notice also that the integrated weight of the thermally excited fluctuations, $\int d\omega \, b(\omega) \text{ Im } D(\omega)$, depends only very weakly on γ.

Resistivity in cuprates. In Fig. 2 we report the experimental data for Nd-La$_{2-x}$Sr$_x$CuO$_4$ and Eu-La$_{2-x}$Sr$_x$CuO$_4$ samples with $x = 0.24$ (from ref. [26], the error bars of the data are smaller than the symbol size), and the resistivity calculated by solving the Boltzmann equation. The scattering rate was obtained from the imaginary part of the electron self-energy, computed at second order in the coupling g between electron quasiparticles and CDFs of the form given by Eq. (1). Details are given in the "Methods" section and in ref. [27].

This calculation follows closely the approach used in ref. [27] for the fermion tight-binding dispersion, the calculation of the electron scattering rate, and the solution of the Boltzmann equation. In particular, we incorporate an elastic scattering rate which is responsible for a finite resistivity at $T = 0$ and which is also always present in the experimental data (note, e.g., that in Fig. 1 of ref. [3], the reported resistivities are the difference with respect to their value extrapolated to $T = 0$).

Regarding the parameters of the fluctuations, these were extracted from RXS experiments on a NdBa$_2$Cu$_3$O$_{7-y}$ sample, consistently leading to a deviation from linearity below
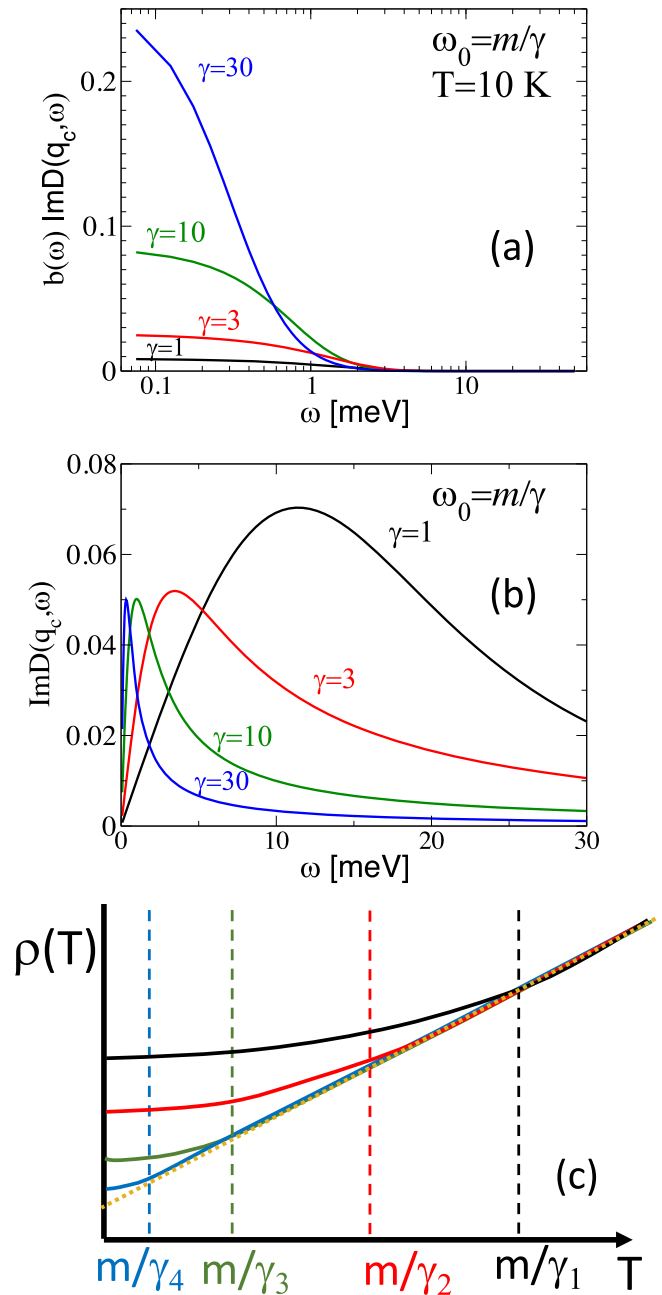

Fig. 1 Implications of the γ parameter. Sketch of the shift induced by an increasing damping parameter $\gamma = 1 \rightarrow 30$ on the fluctuation spectral function Im D in the presence (**a**) and in the absence (**b**) of a Bose thermal distribution; (**c**) sketch of the effect on the resistivity induced by the decrease of the characteristic energy $\omega_0 \equiv m/\gamma$ (with $m = 10$ meV) of the fluctuations responsible for the quasiparticle scattering, with the scattering rate given by the imaginary part of the electron self-energy, computed at second order in the coupling g between electron quasiparticles and fluctuations. The orange dotted line represents the Planckian limit (linearity down to $T = 0$), corresponding to a divergent γ.

$T_{FL} \approx 100$ K in agreement with the resistivity data. Here, we consider the case of Nd-La$_{2-x}$Sr$_x$CuO$_4$, where resistivity under strong magnetic fields is linear down to $T \approx 5$ K. Unfortunately, although RXS experiments recently confirmed also for these cuprates the presence of CDFs with broad momentum distribution[33], detailed data are not available to extract their parameters. This is why we assume here that the parameters fitted from RXS data in NdBa$_2$Cu$_3$O$_{7-y}$ are still reasonable estimates for
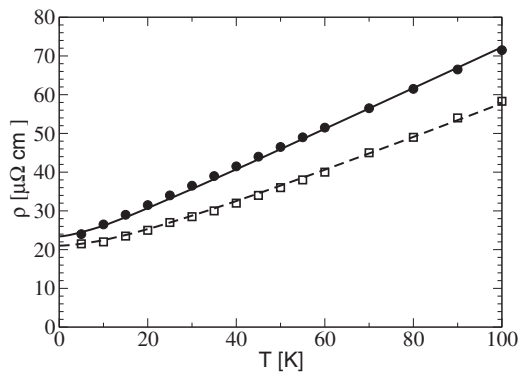
Fig. 2 Linear-in-T resistivity. Resistivity calculations for a Nd-La$_{2-x}$Sr$_x$CuO$_4$ sample with $x = 0.24$ (black solid line) and for a Eu-La$_{2-x}$Sr$_x$CuO$_4$ sample with $x = 0.24$ (black dashed line). The symbols refer to the experimental data extracted from ref. [26] (the error bars of the data are smaller than the symbol size): filled circles for Nd-La$_{2-x}$Sr$_x$CuO$_4$ and empty squares for Eu-La$_{2-x}$Sr$_x$CuO$_4$. For the fitting we used a quasiparticle-charge fluctuations coupling and the elastic scattering rate due to quenched disorder $g^2 = 0.045$ and $\Gamma_0 = 13.7$ meV for Nd-La$_{2-x}$Sr$_x$CuO$_4$ and $g^2 = 0.0415$ and $\Gamma_0 = 12.3$ meV for Eu-La$_{2-x}$Sr$_x$CuO$_4$ (see Methods—the Boltzmann equation and calculation of the electron scattering rate).

Nd-La$_{2-x}$Sr$_x$CuO$_4$ and we therefore use similar values: $m = 10$ meV, $\bar{\nu} = 1.3$ eV (r.l.u.)$^{-2}$, $\bar{\Omega} = 30$ meV. These values correspond to a rather short coherence length of a few lattice spacings, $\xi^{-1} = \sqrt{m/\bar{\nu}} \approx 0.1$ r.l.u.). We reiterate here that such a short coherence length of the CDFs is a crucial feature to obtain a nearly isotropic scattering over the Fermi surface, so that all quasiparticles are nearly equally scattered and their FL properties are uniformly spoiled. As far as the dissipation parameter is concerned, on the basis of the assumption c) given above, we adopt here a phenomenological form for the damping parameter

$$\gamma(p, T) = \left[A/\log\left(1 + T_0/\Theta_T\right) + B|p - p_c| \right]^{-1}, \qquad (2)$$

where $\Theta_T = \min\left(T, \bar{T}\right)$, and $\bar{T}$ sets the temperature scale above which the temperature dependence of γ saturates. Equation (2), with the parameters A, B, and T_0 adjusted to fit resistivity and specific heat data (see below), corresponds to the idea of a damping which increases by decreasing the temperature and is maximal at some doping p_c. The scale $\bar{T}$ is not constrained when fitting the low-temperature specific heat data, and we can only say that $\bar{T} > 10$ K. Eq. (2) implies a dissipative QCP, with a diverging γ at $T = 0$ and $p = p_c$. This translates into the idea that the strange-metal behavior may eventually extend down to $T = 0$: as schematized in Fig. 1(c), an increasingly larger γ extends the linear resistivity to lower and lower temperatures. By consistently fitting the resistivity and specific heat data at various dopings (see below) we determine the parameters $T_0 = 50$ K, $p_c = 0.235$, $A = 0.056$, $B = 0.87$ for Nd-La$_{2-x}$Sr$_x$CuO$_4$, and $T_0 = 37$ K, $p_c = 0.232$, $A = 0.117$, $B = 2.84$ for Eu-La$_{2-x}$Sr$_x$CuO$_4$. We find that the linear resistivity extends down to a few Kelvins for the Nd-La$_{2-x}$Sr$_x$CuO$_4$ sample at $x = 0.24$ (solid black circles and solid black curve in Fig. 2). The data taken in Eu-La$_{2-x}$Sr$_x$CuO$_4$ with x = 0.24 (empty squares and dashed black curve in Fig. 2) seem instead to indicate that this sample is slightly away from the $p \sim p_c$ condition and a deviation from linearity occurs at higher temperatures of a few tens of Kelvins. We point out that, strictly speaking, the so-called Planckian behavior[28,34–39] is a precise way of achieving a linear dependence of the resistivity on the temperature, namely the scattering rate is proportional to the temperature with a prefactor of order one (in units where the Planck and Boltzmann constants are set equal to one). In our

theory, the scattering rate is proportional to the square of the coupling g between electron quasiparticles and fluctuations (see Eq. (5), in "Methods"), which is adjusted to fit the experimental resistivity curves, so our strange-metal behavior is not Planckian, in the sense that does not imply a universal relation between the scattering rate and the temperature. The very issue of the occurrence of a Planckian behavior in cuprates and other systems is controversial and debated[40,41].

Specific heat in cuprates. The phenomenological assumption of a large γ should be validated by investigating its effect on other observables. In particular, since we claim that the main physical effect of large damping is to shift the fluctuation spectral weight to lower energies, it is natural to expect a strong enhancement of the low-temperature specific heat. This is precisely what has been recently observed in other overdoped cuprates[26]. Here we subtract from the observed specific heat the contribution of fermion quasiparticles. Despite the presence of a van Hove singularity, disorder, interplane coupling and electron–electron interactions smoothen this contribution. Thus fermion quasiparticles cannot account for the observed seemingly divergent specific heat.

We argue instead that an enhancement of the boson contribution to the specific heat occurs if γ obeys Eq. (2). The contribution of CDFs to the free energy density is $f_B = \frac{T}{2N} \sum_\ell \sum_q \log\left[\mathcal{D}^{-1}(q, \Omega_\ell)\right]$, where $\mathcal{D}$ is the Matsubara propagator obtained after analytical continuation of Eq. (1), $\Omega_\ell = 2\pi \ell T$, with integer ℓ, and N is the number of unit cells. Hence, we obtain the contribution of damped CDFs to the internal energy density u_B and to the specific heat (details about the derivation are given in the "Methods" section)

$$C_V^B = \frac{\partial u_B}{\partial T} = \frac{\partial}{\partial T} \left[\int_0^\infty \mathrm{d}\omega \, \omega \, b(\omega) \, \rho_B(\omega) \right], \qquad (3)$$

where $\rho_B(\omega)$ plays the role of an effective spectral density, whose full expression is given in the "Methods" section. The low-temperature asymptotic behavior of the specific heat is captured by the low-frequency asymptotic value

$$\rho_B(\omega) \approx \frac{4\gamma}{\bar{\nu}} \log\left(1 + \frac{\bar{\nu}}{4\pi \, m}\right). $$

Figure 3c shows that the enhancement of $\gamma(T, p)$ leading to the observed linear-T behavior in the low-T resistivity, also induces a peak in the specific heat, due to the increase of low-energy boson degrees of freedom. Noticeably, the relative weight (height) of C_V^B at the various temperatures is well captured by our approach. In particular, this feature is mostly ruled by the Bose distribution function in Eq. (3) and depends only little on the specific expression of $\gamma(T, p)$, provided enough spectral density is brought to frequencies $\omega \lesssim T$ with increasing γ. We also notice that the logarithmic temperature dependence of γ mirrors in a nearly logarithmic behavior of C_V/T [see Fig. 3 (a, b)]. We point out that, within our phenomenological approach, it is difficult to estimate the real number of collective charge degrees of freedom contributing to the specific heat, and determine its numerical prefactor. For instance, assuming for the CDFs a correlation length $\xi \approx 1–2$ wavelengths (of order 4–8 lattice units a), one could consider the CDF modes to live on the sites of a coarse-grained lattice. In this way, one could easily estimate that in two dimensions one CDF mode is present on a coarse-grained unit cell whose area may easily be 20–30 times the area of the original microscopic unit cell. This is why the CDF contribution to the specific heat might be rescaled by a seemingly large factor. We also emphasize the crucial difference between scenarios in which the increasing mass of the fermion quasiparticles[42] (as a result e.g. of strong correlations and/or localization) leads to a diverging
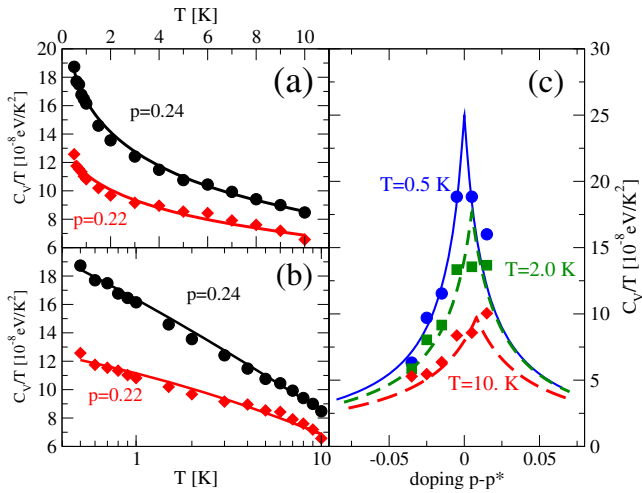
Fig. 3 Specific heat. Temperature dependence of the low-temperature specific heat per unit cell (u.c.) over temperature in Nd–La$_{2-x}$Sr$_x$CuO$_4$ samples with doping $p = 0.24$ (black solid line and circles) and $p = 0.22$ (red solid line and diamonds) in linear (**a**) and semilogarithmic (**b**) [the theoretical curves have been rescaled by an overall factor 1/30, while keeping the relative weight at different doping and temperatures fixed - see the discussion about this prefactor after Eq. (3) in section "Specific heat in cuprates"]. **c** Doping dependence of the low-temperature C_V/T in Nd–La$_{2-x}$Sr$_x$CuO$_4$ samples at different temperatures $T = 0.5, 2.0, 10.0$ K. Symbols represent the experimental data taken from ref. [26], where the related error bars and the discussion of their origin can also be found, while the lines report our theoretical calculations.

specific heat and our theory, where this is due to an increasing damping of the relevant collective modes. Within our approach, the fermion contribution to the specific heat is finite even when γ diverges at $p = p_c$.

Conclusion

The above analysis shows that two nontrivial features of the strange-metal behavior occurring near QCPs can be attributed to, and accounted for by, the damping parameter γ only. We still lack a microscopic scheme to determine the doping and temperature dependence of γ, and, within the scope of the present work, we rely on the phenomenological expression of Eq. (2). Therefore also the $T \log(T_0/T)$ behavior of the specific heat at p_c is only phenomenologically captured by our theory. Nevertheless, we point out that our approach outlines a general paradigmatic change, shifting the relevance from the divergence of the correlation length ξ to the increase (possibly divergence) of dissipation. This is what renders our scheme different from the proposal of a local QCP put forward long ago in ref. [22]. In this latter case the critical behavior of the imaginary part (i.e., damping) of the self-energy of the critical fluctuations, is sublinear $i\gamma_0\omega^{1-\alpha}$, which somehow rephrases our condition of an increasing damping at low energy scales by taking $i(\gamma_0/\omega)^\alpha\omega$ (i.e., $\gamma \sim \gamma_0/\omega^\alpha$), because of a diverging ξ. From our Eq. (2) one can see that the assumption that at $p = p_c$ the scaling index in T for γ is zero, i.e., logarithmically divergent, suggests that $\alpha \to 0$ and the challenge is to obtain this result without $\xi \to \infty$.

After momentum integration, a similar frequency dependence characterizes the singular dynamical interaction between quasiparticles mediated by the critical collective boson, in ref. [43], where a complete analysis of the complementary problem of the competition between pairing and non-FL metal at a QCP is reported.

Of course, other, even more mundane, mechanisms might boost the increase of γ. In cuprates, for instance, p_c occurs at or

very near a van Hove singularity, which enhances the density of states of fermions, thereby increasing the Landau damping γ of the fluctuations. Also the proximity to charge ordering might induce the reconstruction of the Fermi surface[44], thereby triggering an enhanced damping of the CDFs. In any case, while all these mechanisms are worth being explored to shape a microscopic theory of our scenario, it is clear that our phenomenological approach shifts the focus from diverging spacial correlations (and vanishing mass of the fluctuations) to a diverging damping of short-ranged fluctuations, thereby setting a new stage for the violation of the FL behavior.

Methods

The Boltzmann equation. The results for the in-plane resistivity presented in the paper are obtained within a Boltzmann equation approach, following the derivation of ref. [45]. We obtain

$$\frac{1}{\rho} = \frac{e^2}{\pi^3\hbar}\frac{2\pi}{d}\int d\phi \; \frac{k_F(\phi)v_F(\phi)\cos^2(\phi-\eta)}{\Gamma(\phi)\cos(\eta)} \;, \tag{4}$$

where $k_F(\phi)$, $v_F(\phi)$, and $\Gamma(\phi)$ denote the angular dependence of the Fermi momentum, Fermi velocity, and scattering rate along the Fermi surface and

$$\eta = \text{atan}\left(\frac{1}{k_F}\frac{\partial k_F}{\partial\phi}\right).$$

The scattering rate $\Gamma(\phi) \equiv \Gamma_0 + \Gamma_\Sigma(\phi)$ includes an elastic scattering rate Γ_0, and the scattering rate due to CDFs, $\Gamma_\Sigma(\phi) \equiv -\text{Im } \Sigma(k_F(\phi), \omega = 0)$, where $\Sigma(\mathbf{k}, \omega)$ is the electron self-energy [see ref. [27] and its Supplementary Information].

The electron dispersion ε_k includes nearest-, next-nearest- and next-next-nearest-neighbor hopping terms generic for cuprates[46]. The c-axis lattice constant for Nd-LSCO is taken as $d \approx 11$ Å.

Calculation of the electron scattering rate. To obtain the electron scattering rate needed to calculate the electric transport, we carried out a perturbative calculation of the self-energy corrections of the fermion quasiparticles using the Feynman diagram of Fig. 4, where the solid line represents a bare quasiparticle, and the wavy line represents a CDF collective excitation.

The analytic expression for the (retarded) imaginary part is[27]

$$\text{Im } \Sigma(\mathbf{k}, \omega) = -g^2\int\frac{d^2\mathbf{q}}{(2\pi)^2}$$
$$\times \frac{(\omega-\varepsilon_{\mathbf{k-q}})[b(\varepsilon_{\mathbf{k-q}})+f(\varepsilon_{\mathbf{k-q}}-\omega)]}{[\omega_0+\bar{\nu}\eta_{\mathbf{q}}-(\omega-\varepsilon_{\mathbf{k-q}})^2/\overline{\Omega}]^2+(\omega-\varepsilon_{\mathbf{k-q}})^2}, \tag{5}$$

where $b(z) = [e^{z/k_BT}-1]^{-1}$ is the Bose function, $f(z) = [e^{z/k_BT}+1]^{-1}$ is the Fermi function, g is the coupling between electrons and CDFs and $\eta_q = 4-2\cos(q_x-Q_x^c)-2\cos(q_y-Q_y^c)$ contains the information about the CDF vector $\mathbf{q}_c$. The parameter $\bar{\nu}$ should be scaled by $1/(2\pi)^2$ ($\bar{\nu} \to \bar{\nu}/(4\pi^2)$) if the momenta are given in r.l.u. as it is customary, e.g., in RXS experiments (see also below in the calculation of the specific heat). For the evaluation of $\Gamma_\Sigma \equiv \text{Im } \Sigma(k_F, 0)$ we sum over all 4 equivalent wavevectors ($\pm q_c, 0$) and ($0, \pm q_c$), with $q_c \approx 0.3$ r.l.u.

Calculation of the specific heat. To define the specific heat contribution from a collective mode with finite lifetime we start from the free energy of a free boson in terms of its inverse propagator $\mathcal{D}^{-1}$ and we determine the effect of γ, by calculating the excess free energy

$$\delta\mathcal{F} = \frac{1}{2\beta}\sum_{n,\mathbf{q}}\left[\log\left(\frac{\omega_n^2}{\overline{\Omega}}+\gamma|\omega_n|+\omega_{\mathbf{q}}\right)-\log\left(\frac{\omega_n^2}{\overline{\Omega}}+\omega_{\mathbf{q}}\right)\right].$$

Here, the second term represents the free energy of undamped "phonons" with dispersion $(\overline{\Omega}\omega_{\mathbf{q}})^{1/2}$, which is subtracted to eliminate the most divergent term in the Matsubara frequency sum. The corresponding excess of internal energy is given

by $\delta\mathcal{U} = \frac{\partial}{\partial\beta}(\beta\,\delta\mathcal{F})$, (with $\beta = \frac{1}{k_B T}$) finding

$$\delta\mathcal{U} = k_B T \sum_{n,\mathbf{q}} \left[\frac{\omega_{\mathbf{q}} + \frac{1}{2}\gamma|\omega_n|}{\frac{\omega_n^2}{\Omega} + \gamma|\omega_n| + \omega_{\mathbf{q}}} - \frac{\omega_{\mathbf{q}}}{\frac{\omega_n^2}{\Omega} + \omega_{\mathbf{q}}} \right]. \tag{6}$$

This expression allows us to define the internal energy of the damped CDFs as

$$\mathcal{U} = k_B T \sum_n \sum_{\mathbf{q}} \frac{\omega_{\mathbf{q}} + \frac{1}{2}\gamma|\omega_n|}{\frac{\omega_n^2}{\Omega} + \gamma|\omega_n| + \omega_{\mathbf{q}}}.$$

The Matsubara sum of the term with $\frac{1}{2}\gamma|\omega_n|$ in the numerator is formally divergent and therefore a convergency factor should be included as it is customary in diagrams with closed loops. By introducing the spectral representation of the boson propagator, and carrying out the Matsubara sum, the thermal part of the internal energy is obtained as

$$\mathcal{U} = \sum_{\mathbf{q}} \frac{1}{\pi} \int_0^\infty \mathrm{d}\omega \; \frac{\gamma\omega\left(\frac{\omega^2}{\Omega} + \omega_{\mathbf{q}}\right)}{\left(\frac{\omega^2}{\Omega} - \omega_{\mathbf{q}}\right)^2 + \gamma^2\omega^2} \; b(\omega).$$

The specific heat is obtained by differentiating the internal energy with respect to T and dividing by the size of the system (e.g., the number N of unit cells), yielding

$$C_V^B = \frac{\partial}{\partial T} \int_0^\infty \mathrm{d}\omega \; \rho_B(\omega) \; \omega \; b(\omega), \tag{7}$$

where an effective density of states

$$\rho_B(\omega) = \frac{1}{N} \sum_{\mathbf{q}} \frac{1}{\pi} \frac{\gamma\left(\frac{\omega^2}{\Omega} + \omega_{\mathbf{q}}\right)}{\left(\frac{\omega^2}{\Omega} - \omega_{\mathbf{q}}\right)^2 + \gamma^2\omega^2}$$

has been defined.

We consider a three-dimensional unit cell, but we assume that the dispersion in $\vec{q}$-space is only on the x, y plane. Introducing a density of states for the variable $\bar{\nu}|\vec{q} - \vec{q}_c|^2$,

$$g(\varepsilon) = \frac{1}{N} \sum_{\mathbf{q}} \delta(\bar{\nu}|\vec{q} - \vec{q}_c|^2 - \varepsilon) \approx \frac{1}{\pi\bar{\nu}}\theta(\Lambda - \varepsilon),$$

where, in order to find an analytical expression, we approximate the quarter of the Brillouin zone with a circle centered at each of the four equivalent $\vec{q}_c$, with radius $\bar{q}$, and $\Lambda \approx \bar{\nu}\bar{q}^2$. We then obtain the analytical expression of the effective spectral density of the CDF

$$\rho_B(\omega) = \frac{\gamma}{2\pi^2\bar{\nu}} \log \frac{\left(m + \Lambda - \frac{\omega^2}{\Omega}\right)^2 + \gamma^2\omega^2}{\left(m - \frac{\omega^2}{\Omega}\right)^2 + \gamma^2\omega^2}$$

$$+ \frac{2\omega}{\pi^2\bar{\nu}\,\Omega} \left[\arctan\left(\frac{m+\Lambda}{\gamma\omega} - \frac{\omega}{\gamma\Omega}\right) - \arctan\left(\frac{m}{\gamma\omega} - \frac{\omega}{\gamma\Omega}\right) \right]. \tag{8}$$

Since we are considering the limit of low temperatures it is reasonable to assume both $\omega \ll \sqrt{\Omega(m+\Lambda)}$ and $\gamma\omega \ll m + \Lambda$. In this regime, we can approximate $\rho_B(\omega)$ as $\rho_B(\omega) \approx \frac{\gamma}{\pi^2\bar{\nu}} \log\left(1 + \frac{\Lambda}{m}\right)$. If one uses r.l.u., then the replacement $\bar{\nu} \to \bar{\nu}/(4\pi^2)$ must be performed, and one finds the expression for the low-frequency asymptotic behavior of $\rho_B(\omega)$ given in the main text.

The approximation becomes more and more accurate at lower and lower temperature. From this equation it is evident that $\rho_B(\omega)$ is a linear function of γ, and so is the specific heat. Since $\rho_B(\omega)$ is a constant function of ω in the regime of our interest, we get the explicit expression

$$C_V^B \approx \frac{\gamma}{\pi^2\bar{\nu}} \log\left(1 + \frac{\Lambda}{m}\right) \frac{\partial}{\partial T}\left(k_B^2 T^2 \int_0^\infty \frac{x}{e^x - 1} \mathrm{d}x \right).$$

Our final expression for the ratio C_V^B/T is then

$$\frac{C_V^B}{T} \approx k_B^2 \frac{\gamma}{3\bar{\nu}} \log\left(1 + \frac{\pi\bar{\nu}}{m}\right).$$

Again, if one uses r.l.u., the substitution $\bar{\nu} \to \bar{\nu}/(4\pi^2)$ must be performed.

Data availability

Data sharing not applicable to this article as no datasets were generated or analysed during the current purely theoretical work The data reported in Figs. 2, 3 have been extracted from ref. [26].

Code availability

The theoretical analysis was carried out with FORTRAN codes to implement various required numerical integrations appearing in the Boltzmann equation, cf. "Methods", and for the evaluation of the specific heat, cf. Eq. (3). Although the same task could easily be performed with Mathematica or other standard softwares, the used FORTRAN codes are available from one of the corresponding authors [M.G.] on reasonable request.

References

1. Stewart, G. R. Non-Fermi-liquid behavior in d- and f-electron metals. *Rev. Mod. Phys.* **73**, 797 (2001).
2. Walmsley, P. et al. Quasiparticle mass enhancement close to the quantum critical point in BaFe$_2$(As$_{1-x}$P$_x$)$_2$. *Phys. Rev. Lett.* **110**, 257002 (2013).
3. Legros, A. et al. Universal T-linear resistivity and Planckian dissipation in overdoped cuprates. *Nat. Phys.* **15**, 142 (2019).
4. Bruin, J. A. N., Sakai, H., Perry, R. S. & Mackenzie, A. P. Similarity of scattering rates in metals showing T-linear resistivity. *Science* **339**, 804 (2013).
5. Anderson, P. W. *The Theory of Superconductivity in the High Temperature Cuprates* (Princeton University Press, 1997).
6. Kastrinakis, G. A. Fermi liquid model for the overdoped and optimally doped cuprate superconductors: scattering rate, susceptibility, spin resonance peak and superconducting transition. *Physica C* **340**, 119 (2000).
7. Sachdev, S., *Quantum Phase Transitions* Ch 12 (Cambridge University Press, 1999).
8. Hertz, J. A. Quantum critical phenomena. *Phys. Rev. B* **14**, 1165 (1976).
9. Millis, A. J. Effect of a non-zero temperature on quantum critical points in itinerant fermion systems. *Phys. Rev. B* **48**, 7183 (1993).
10. Castellani, C., Di Castro, C. & Grilli, M. Non-Fermi-liquid behavior and d-wave superconductivity near the charge-density-wave quantum critical point. *Z. Phys. B* **103**, 137 (1996).
11. Castellani, C., Di Castro, C. & Grilli, M. Singular quasiparticle scattering in the proximity of charge instabilities. *Phys. Rev. Lett.* **75**, 4650 (1995).
12. Caprara, S., Di Castro, C., Seibold, G. & Grilli, M. Dynamical charge density waves rule the phase diagram of cuprates. *Phys. Rev. B* **95**, 224511 (2017).
13. Arpaia, R. et al. Dynamical charge density fluctuations pervading the phase diagram of a Cu-based high-T$_c$ superconductor. *Science* **365**, 906 (2019).
14. Fidrysiak, M. & Spalek, J. Unified theory of spin and charge excitations in high-Tc cuprate superconductors: a quantitative comparison with experiment and interpretation. *Phys. Rev. B* **104**, L020510 (2021).
15. Nag, A. et al. Detection of acoustic plasmons in hole-doped lanthanum and bismuth cuprate superconductors using resonant inelastic X-ray scattering. *Phys. Rev. Lett.* **125**, 257002 (2020).
16. Castellani, C., Di Castro, C. & Metzner, W. Instabilities of anisotropic interacting Fermi systems. *Phys. Rev. Lett.* **69**, 1703 (1992).
17. Hlublina, R. & Rice, T. M. Resistivity as a function of temperature for models with hot spots on the Fermi surface. *Phys. Rev. B* **51**, 9253 (1995).
18. Rosch, A. Interplay of disorder and spin fluctuations in the resistivity near a quantum critical point. *Phys. Rev. Lett.* **82**, 4280 (1999).
19. Brando, M., Belitz, D., Grosche, F. M. & Kirkpatrick, T. R. Metallic quantum ferromagnets. *Rev. Mod. Phys.* **88**, 025006 (2016).
20. Aji, V. & Varma, C. M. Theory of the quantum critical fluctuations in cuprate superconductors. *Phys. Rev. Lett.* **99**, 067003 (2007).
21. Dell'Anna, L. & Metzner, W. Electrical resistivity near Pomeranchuk instability in two dimensions. *Phys. Rev. Lett.* **98**, 136402 (2007).
22. Si, Q., Rabello, S., Ingersent, K. & Smith, J. Locally critical quantum phase transitions in strongly correlated metals. *Nature* **413**, 804 (2001).
23. Coleman, P., Pépin, C., Si, Q. & Ramazashvili, R. How do Fermi liquids get heavy and die? *J. Phys.: Condens. Matter* **13**, R723 (2001).
24. Burdin, S., Grempel, D. R. & Grilli, M. A large-N analysis of the local quantum critical point and the spin-liquid phase. *Phys. Rev. B* **67**, 121104(R) (2003).
25. Patel, A. A., McGreevy, J., Arovas, D. P. & Sachdev, S. Magnetotransport in a Model of a Disordered Strange Metal. *Phys. Rev. X* **8**, 021049 (2018).
26. Michon, B. et al. Thermodynamic signatures of quantum criticality in cuprate superconductors. *Nature* **567**, 218222 (2019).
27. Seibold, G. et al. Strange metal behaviour from charge density fluctuations in cuprates. *Commun. Phys.* **4**, 7 (2021).
28. Zaanen, J. Why the temperature is high. *Nature* **430**, 512 (2004).
29. Girod, C. et al. Normal state specific heat in the cuprates La$_{2-x}$Sr$_x$CuO$_4$ and Bi$_{2+y}$Sr$_{2-x-y}$La$_x$CuO$_{6+\delta}$ near the critical point of the pseudogap phase. *Phys. Rev. B.* 103 https://doi.org/10.1103/PhysRevB.103.214506 (2021).
30. Andergassen, S., Caprara, S., Di Castro, C. & Grilli, M. Anomalous isotopic effect near the charge-ordering quantum criticality. *Phys. Rev. Lett.* **87**, 056401 (2001).
31. Caprara, S., Di Castro, C., Fratini, S. & Grilli, M. Anomalous optical absorption in the normal state of overdoped cuprates near the charge-ordering instability. *Phys. Rev. Lett.* **88**, 147001 (2002).
32. Caprara, S., Grilli, M., Di Castro, C. & Enss, T. Optical conductivity near finite-wavelength quantum criticality. *Phys. Rev. B* **75**, 140505(R) (2007).
33. Miao, H. et al. Charge density waves in cuprate superconductors beyond the critical doping. *npj Quantum Mater.* **6**, 31 (2021).
34. Hartnoll, S. A. & Mackenzie, A. P. Planckian dissipation in metals. https://arxiv.org/abs/2107.07802v1 (2107).

35. Bruin, J. A. N., Sakai, H. & Mackenzie, A. P. Similarity of scattering rates in metals showing T-linear resistivity. *Science* **339**, 804 (2013).
36. Zaanen, J. Planckian dissipation, minimal vsicosity and the transport in cuprate strange metals. *SciPost Phys.* **6**, 061 (2019).
37. Patel, A. A. & Sachdev, S. Theory of a Planckian metal. *Phys. Rev. Lett.* **123**, 066601 (2019).
38. Dumitrescu, P. T., Wentzell, N., Georges, A. & Parcollet, O. Planckian metal at a doping-induced quantum critical point. Preprint at https://arxiv.org/abs/2103.08607.
39. Mousatov, C. H., Berg, E. & Hartnoll, S. A. Theory of the strange metal $Sr_3Ru_2O_7$. *Proc. Natl Acad. Sci.* **117**, 2852 (2020).
40. Hwang, E. W. & Das Sarma, S. Linear-in T resistivity in dilute metals: a Fermi liquid perspective. *Phys. Rev. B* **99**, 085105 (2019).
41. Sadovskii, M. V. Planckian relaxation delusion in metals. *Phys.—Usp.* **64**, 175 (2021).
42. Ramshaw, B. J. et al. Quasiparticle mass enhancement approaching optimal doping in a high-T_c superconductor. *Science* **348**, 317 (2015).
43. Abanov, A. & Chubukov, A. V. Interplay between superconductivity and non-Fermi liquid at a quantum critical point in a metal. I. The γ model and its phase diagram at $T = 0$: The case $0 < \gamma < 1$. *Phys. Rev. B* **102**, 024524 (2020).
44. Badoux, S. et al. Change of carrier density at the pseudogap critical point of a cuprate superconductor. *Nature* **531**, 210 (2016).
45. Hussey, N. E. The normal state scattering rate in high-T_c cuprates. *Eur. Phys. J. B* **31**, 495 (2003).
46. Meevasana, W. et al. Hierarchy of multiple many-body interaction scales in high-temperature superconductors. *Phys. Rev. B* **75**, 174506 (2007).

Acknowledgements

Author contributions

S.C., C.D.C., and M.G. conceived the project. G.M. performed the theoretical calculations of the resistivity and specific heat, with contributions from G.S., S.C., C.D.C., and M.G. The manuscript was written by S.C., C.D.C., M.G., G.S., with contributions and suggestions from G.M.

Competing interests

The authors declare no competing interests.

Additional information

Supplementary information The online version contains supplementary material available at https://doi.org/10.1038/s42005-021-00786-y.

Correspondence and requests for materials should be addressed to Sergio Caprara or Marco Grilli.

Peer review information *Communications Physics* thanks the anonymous reviewers for their contribution to the peer review of this work. Peer reviewer reports are available.

Reprints and permission information is available at http://www.nature.com/reprints

Publisher's note Springer Nature remains neutral with regard to jurisdictional claims in published maps and institutional affiliations.